

# Seismic Evaluation and Post-earthquake Safety Assessment of Gravity Dam Based on Numerical Simulation

**A. Iliev, K. Apostolov, A. Andonov & S. Andreev**

*Risk Engineering Ltd, Sofia, Bulgaria*

**M. Kostov & G. Varbanov**

*National Institute in Geophysics, Geodesy and Geography, Bulgarian Academy of Sciences*



## SUMMARY:

In the current paper an exemplary gravity dam, constructed in the 1950s and situated in a seismically active region, is investigated for various seismic levels. Three-dimensional FE model is developed, including the surrounding rock foundation and dynamic analyses are performed for various seismic levels. The nonlinear behaviour of concrete is modelled with the Ottosen constitutive law representing the realistic material behaviour using the smeared crack approach. The critical zones of the dam and the accumulated damages are identified. The damage states are “rated” based on predefined Damage Levels (DL) according to their safety significance. Additional analyses are performed assessing the post-earthquake stability of the dam.

*Keywords: Post-earthquake Safety Assessment, Gravity Dam, Damage Indicator Parameters, Seismic Safety*

## 1. INTRODUCTION

The history of the large dam accidents shows that the gravity dams are more vulnerable and accumulate more and heavier damages than the arch dams. Particular attention should be paid to gravity dams constructed up to the late decades of the last century when mainly simplified methods were used for seismic assessment of the dam structure. The increased safety criteria nowadays lead to necessity of seismic reassessment of the important infrastructures, particularly those whose economic impact in case of failure is enormous.

In the present study a seismic investigation of an exemplary concrete gravity dam, constructed in the middle of the last century is carried out. The dam is situated in a region with high seismic intensity and the input records, representing the different seismic levels, are based on a site-specific seismic hazard assessment. During the construction period the dam site was considered with low seismicity, however recent investigation shows a higher potential for generation of strong seismic events. For the purpose of the seismic safety assessment a detailed finite element model is used, representing the exact geometry of the dam including the surrounding rock foundation. The material properties of the concrete and the rock layers are obtained from various laboratory and in-situ tests carried out. The thermal stressed and deformed state of the wall is taken into account in the performed analyses.

The structural response of the dam is evaluated based on series of nonlinear dynamic analysis, representing the seismic levels including OBE, MCE and beyond design levels. Predefined Damage Levels (DL) are used for rating of the accumulated damages after the seismic impact and assessment of the overall damaged state. The obtained damages and critical zones of the dam are outlined and correlated to the different Damage Levels. Additionally various motion parameters (CAV,  $S_a$ , PGA) for each seismic level are traced and subsequently associated with the predefined Damage Levels.

## 2. DESCRIPTION OF THE STRUCTURE AND THE REGIONAL SEIZMICITY

The selected dam is a concrete gravity dam composed of 18 separate blocks. The general geometrical properties of the dam are:

- total crest length ~ 200 m;
- maximum height ~ 70 m;
- width of crest ~ 7 m;
- maximum width of base ~ 60m;
- total volume of the wall – about 200000m<sup>3</sup>.

The spillway is situated in the two central blocks of the dam. A total of four galleries are available in the dam structure: one injection gallery, two inspection galleries and one transverse gallery. The grouting curtain is located under the injection gallery at the upstream part of the dam and its depth varies between 18 and 50 meters. General view of the dam wall and a vertical cross section of a central block are presented in Fig. 2.1.

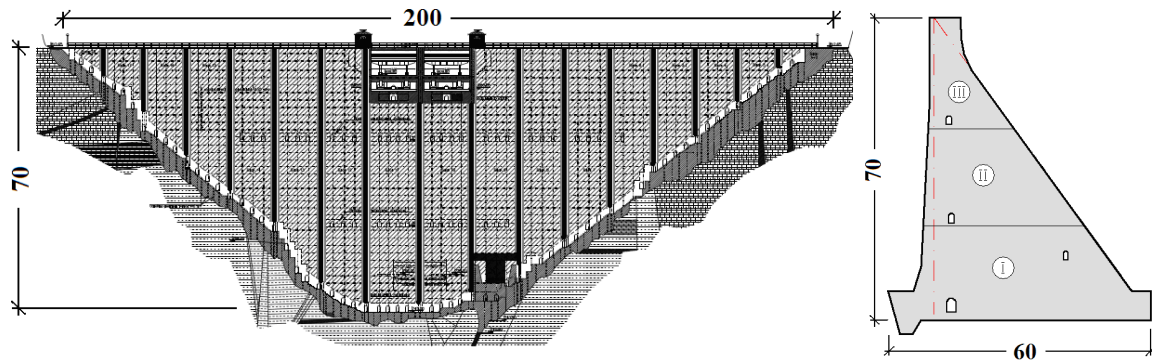


**Figure 2.1.** General view and vertical cross section of the dam

A number of geological surveys, laboratory tests and in-situ measurements are carried out to obtain and verify the material properties of the mass concrete and the rock foundation at the dam site. The initial design of the dam prescribed three different concrete type groups along the dam's height. The concrete of higher grade and more water-impermeable was used for the lower parts of the dam, see Fig. 2.1. The current laboratory tests and in-situ investigations proved this concrete grade distribution.

All statistical results for the static concrete properties were derived from the laboratory tests of a number of concrete samples along the dam's height. The dynamic E-modulus of the different concrete zones was explicitly obtained from the results of seismic tomography performed for the dam structure. Based on these results, regions with decreased dynamic E-modulus were detected at the upstream part of the dam structure. The statistics of the material parameters of the rock foundation layers were obtained based on the results of the laboratory tests of rock samples extracted from the made boreholes.

To assess the seismic activity of the dam region a site-specific seismic hazard assessment was performed, taking into account all regional seismic sources. Four seismic levels are determined for the present study, depending on their return period, including OBE (Operational Basis Earthquake), MCE (Maximum Credible Earthquake) and two seismic excitations with lower probability of exceedance. The PGA of all used seismic levels are compatible with the median PSHA results with the respective probability of exceedance. Each seismic level is presented by a set of three statistically-independent accelerograms, matching the uniform hazard acceleration response spectrum for given return period. The selected seismic levels are presented in Table 2.1.

**Table 2.1.** Seismic levels and respective Peak Ground Accelerations

| Seismic Level | Return Period (years) | PGA (g) |
|---------------|-----------------------|---------|
| A (OBE)       | 1000                  | 0,2     |
| B (MCE)       | 10 000                | 0,35    |
| C             | 100 000               | 0,6     |
| D             | 1 000 000             | 0,9     |

### 3. FINITE ELEMENT MODEL AND ANALYSES DETAILS

A complex three-dimensional finite element model including the dam and the surrounding rock foundation is used for assessments the structural response under seismic excitation. The dam model is consisted of nearly 70 000 mainly prismatic solid elements and the rock foundation model – around 30 000 tetrahedral solid elements. Average size of the solid element of the dam structure is approximately 2m. The exact geometry of the dam, the spillway and location of the galleries are taken into account in the modelling. The foundation part and the base joint plane are presented accounting their real geometry. The modelling of the rock foundation is consistent with the recommendations in various engineering standards and guidelines and is assumed to be one dam’s height in all three directions around the dam structure. The contact between the separate blocks is modelled by finite elements with adjusted material properties which provide on one hand possibility for cantilever behaviour of the separate blocks in case of open contraction joints and on another – absence of discontinuity of the model and stability of the numerical analyses. The boundary conditions of the whole model restrict the translational displacements of the nodes of all lateral sides of the rock foundation model. The general view of the FE model is shown in Fig. 3.1.

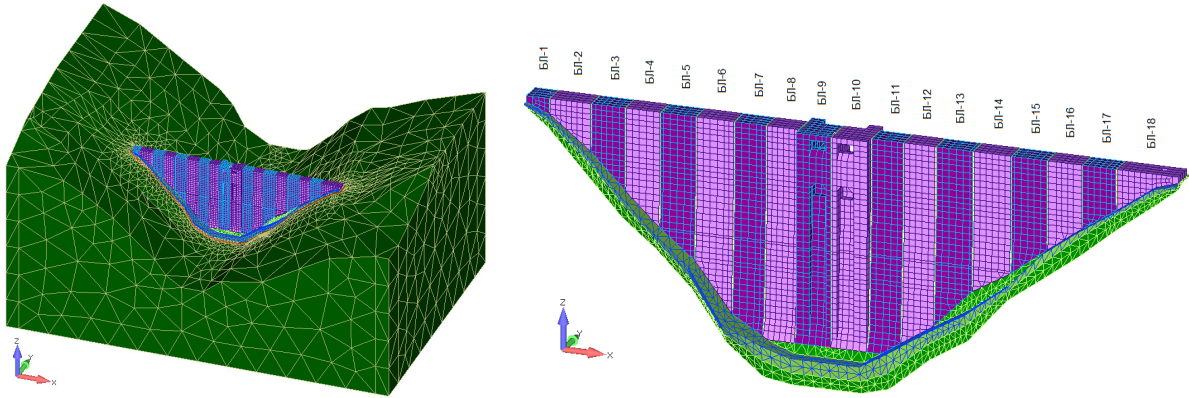


Figure 3.1. Finite element dam model with the rock foundation.

The dynamic analyses are performed using the FEM code SOLVIA. A nonlinear concrete material model is used for the dam body, the base joint and the contraction joint. The concrete constitutive law model, implemented in SOLVIA is based on the Ottosen concrete model and allows realistic material behaviour representation using the smeared crack approach. The uniaxial stress-strain curve of the concrete model is shown in Fig. 3.2.

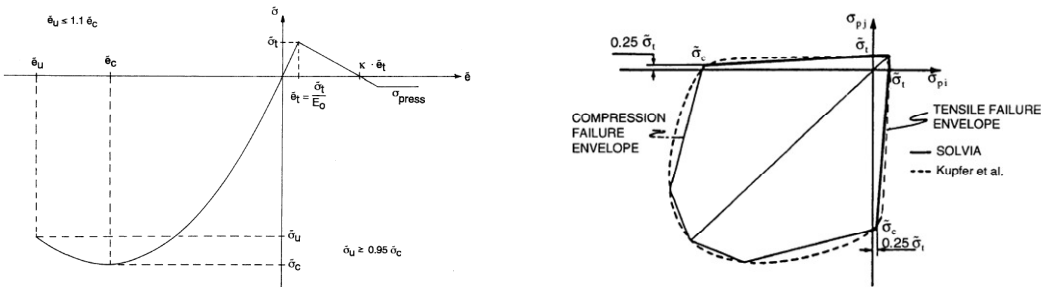
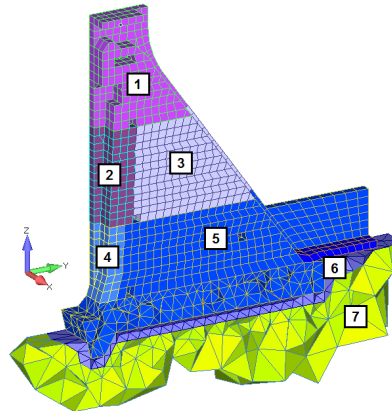


Figure 3.2. Uniaxial stress-strain curve and failure envelope for concrete, used in SOLVIA

The material properties for the dam and the foundation are based on the laboratory and in-situ tests. The concrete material distribution in the dam structure is shown in Fig. 3.3. The results of the seismic tomography indicated decreased dynamic E-modulus in the middle and bottom part of the upstream region. These regions are illustrated as 2 and 4.



**Figure 3.3.** Different concrete materials distributed in the dam structure

The strength material properties are obtained from the laboratory tests results using the 95% fractile of their statistical distribution. The dynamic tensile strength of concrete is assumed to be 50% higher than the static one and the dynamic compressive strength of concrete is assumed to be 15% higher than the static (FERC, 2002). The tests for the rock foundation material indicated higher strength values compared with the concrete material. The rock foundation is presented in the model as elastic and massless medium.

The base joint is modelled as a layer of finite elements with decreased dynamic tensile strength, assuming it to be 55% of the dynamic tensile strength of lower zone concrete (FERC, 2002). The behaviour of the contraction joints between the blocks is represented by a thin layer of finite elements with substantially reduced tensile strength and shear stiffness, thus properly simulating the frictional interaction in case of closed contraction joints. All material properties used in the model are presented in Table 3.1.

**Table 3.1.** Material properties used in the model

| Material            | $E_{dyn}$<br>MPa | $R_{t, dyn}$<br>MPa | $R_{c, dyn}$<br>MPa | Poisson<br>ratio |
|---------------------|------------------|---------------------|---------------------|------------------|
| Concrete zones      |                  |                     |                     |                  |
| 1                   | 12500            | 1,50                | 18,00               | 0,28             |
| 2                   | 9000             | 1,55                | 22,00               | 0,29             |
| 3                   | 13500            | 1,55                | 22,00               | 0,29             |
| 4                   | 9000             | 2,00                | 27,00               | 0,28             |
| 5                   | 21000            | 2,00                | 27,00               | 0,26             |
| Base joint (6)      | 21000            | 1,10                | 27,00               | 0,26             |
| Rock Foundation (7) | 24000            | ---                 | ---                 | 0,35             |

The initial stress-strain state of the dam for the seismic impact analysis is based on self weight, hydrostatic pressure and thermal-stress analysis. The hydrostatic pressure is applied as element pressure, normal to the outer face of all upstream dam elements, assumed to be average annual water level. Uplift pressure is applied at the bottom surface elements of the model taking into account the piezometric measurements.

The hydrodynamic water pressure is represented using the Westergaard method. The calculated masses are applied as lumped masses to all the nodes on the upstream side of the dam under the water level. The distributed added masses for central and lateral block of the dam are presented in Fig. 3.4.

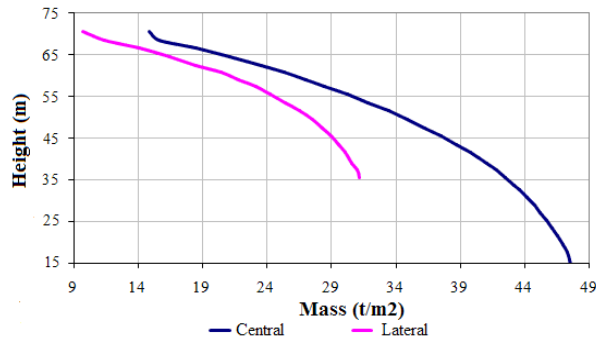


**Figure 3.4.** Distributed added masses for central and lateral block

The transient temperature analysis is based on the annual temperature curves for the air and various water layers in depth. The temperature curves are obtained from the available monitoring data for the dam region see Fig. 3.5. For the initial stress-strain condition of the dam it is conservatively assumed the temperature period when the opening of the contraction joints between the blocks is maximal.

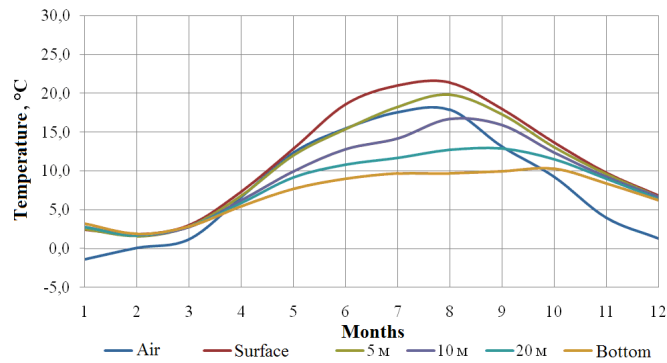


**Figure 3.5.** Temperature curves for air and various water layers

As indicated above the input motion records for the different seismic levels are based on the site-specific PSHA. The PGA of the seismic motion in vertical direction is assumed 90% of the motion in horizontal direction. For the accelerograms generation is applied the approach of modification of a number of real strong-motion records to match the target spectrum for each seismic level. This approach is more realistic and the parameters of the generated seismic excitations are more accurately presented. An exemplary input record and its compatibility with the target spectrum is shown on Fig. 3.6.

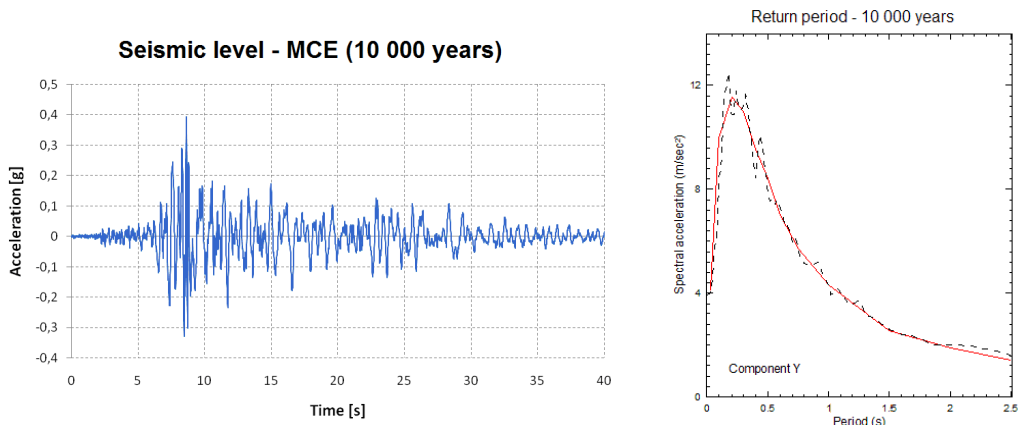


**Figure 3.6.** Seismic excitation for level MCE (10 000 years) and its compatibility with the target spectrum

## 4. RESULTS

### 4.1. Verification of the computational model

One possible validation of the computational model is the comparison of the deformability of the dam from the annual temperature changes influencing the dam's structure. A transient numerical simulation of the stressed and strained state of the structure is performed, exposed on the air and water annual temperature changes and hydrostatic load. The results from the analysis are compared with the results obtained through the monitoring system installed at the dam wall. The selected parameter for the results comparison is horizontal displacement at the top of the crest. At the dam these displacements are measured by the plump bob installed in the structure. The comparison of the results obtained from the monitoring system and the computational model are presented in Fig. 4.1. The results show reliable proximity between the real and the simulated displacements as the maximum difference is less than 15%.

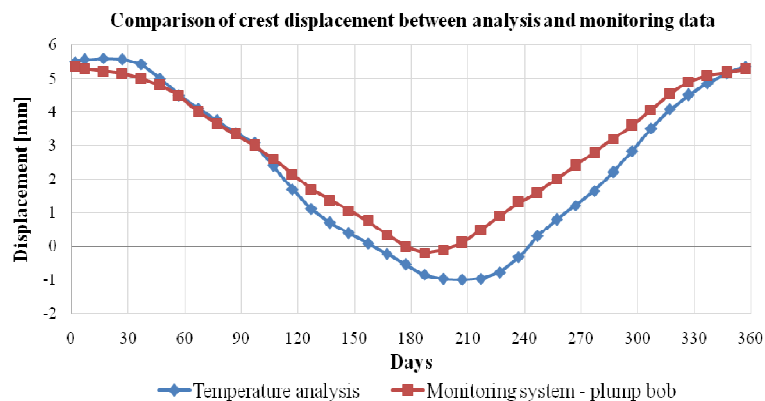


Figure 4.1. Comparison between analysis and monitoring horizontal displacements at the crest

### 4.2. Damaged States for different Seismic Levels

Five Damage Levels (DL) are defined, based on engineering judgment and various engineering guidelines. The DL represent different states of accumulated damages of the dam from initial superficial cracks to total failure. Short description of the Damage Levels is presented below:

**DL0** – elastic response; no cracks expected for the structure;

**DL1** – superficial cracking to initial structural damages; minor inelastic structural response;

**DL2** – initial to moderate structural damages; moderate inelastic structural response; possibility for significant cracks in the structure; damage inspection should be performed

**DL3** – moderate to heavy structural damages; significant inelastic structural response; possibility for cracks passing through the whole dam cross section; decrease of water level and subsequent inspection

**DL4** – heavy structural damages to total failure; heavy inelastic structural response and possibility for loss of structural integrity; evacuation of local communities is necessary and immediate decrease of water level

Four seismic levels are investigated in the present study, ranging from A to D (depending on their return period), as level A represents OBE, level B – MCE and level 3 and 4 are beyond design earthquakes. During all seismic excitations, the most active dynamic behavior is predominantly at the upper third of the central 4 to 8 blocks of the dam. Therefore, this is the zone that accumulates greater damages compared to the rest of the structure. The description of the accumulated damages during and after each seismic level is exposed herein and relation of the damaged states with DL is performed. The damage distribution for the cross section of a central block for all selected earthquake levels is presented in Fig. 4.2.

### Seismic level A (OBE)

Minor cracks are observed at the pilasters from the upstream side of the dam that could be classified as micro-cracks having no influence on the bearing capacity and negligible effect on the initial stiffness of the system. The response of the wall during this seismic level can be assumed as practically within the elastic range. Since the wall has not changed its bearing capacity, the damaged state of the dam could be classified as **DL1**, i.e. no risk for the bearing capacity of the wall and the population along the river bed.

### Seismic level B (MCE)

The accumulated damages at the wall after seismic event of level B (MCE) are concentrated at the upper third of the wall, close to the second inspection gallery downward. Cracks on both upstream and downstream sides of the dam are observed. The cracks at the upstream side are initiated around the level of the gallery while the crack at the downstream side is initiated around 6-8 meters higher. During the analysis the both side cracks tend to propagate into the dam wall perpendicularly to upstream and downstream side. At the end of the excitation record both cracks propagated nearly through the whole cross section of the dam meeting near the inspection gallery. The damage locations are consequence of the active response of the crest, the weakened cross section due to the inspection gallery and the lower concrete strength at the upper part of the wall. In the dam's longitudinal direction the crack is spread among the four middle blocks of the wall. Eventual formation of such crack passing through the whole cross section could lead to a detachment of the upper part of the crest, and will have major priority on the categorization of the status of the dam after an earthquake of level MCE. The damage state could be categorized as **DL2** to **DL3** and post-earthquake sliding and overturning stability of the detached part should be proved.

### Seismic level C

The crack formation at the upper part of the dam is at similar location as in case of seismic level B. However the formed crack in this case is horizontal and passes through the whole cross section of the wall. Another crack perpendicular to the upstream side is formed at the middle of the wall passing through the half of the wall width. The damages in the dam are significantly more than in case of seismic level B, however the additional damages are located at the downstream side and will not lead to additional uncontrolled leakage. The categorization of the post-earthquake condition of the dam – **DL3** or **DL4**, again will depend mainly on the post-earthquake stability of the detached part.

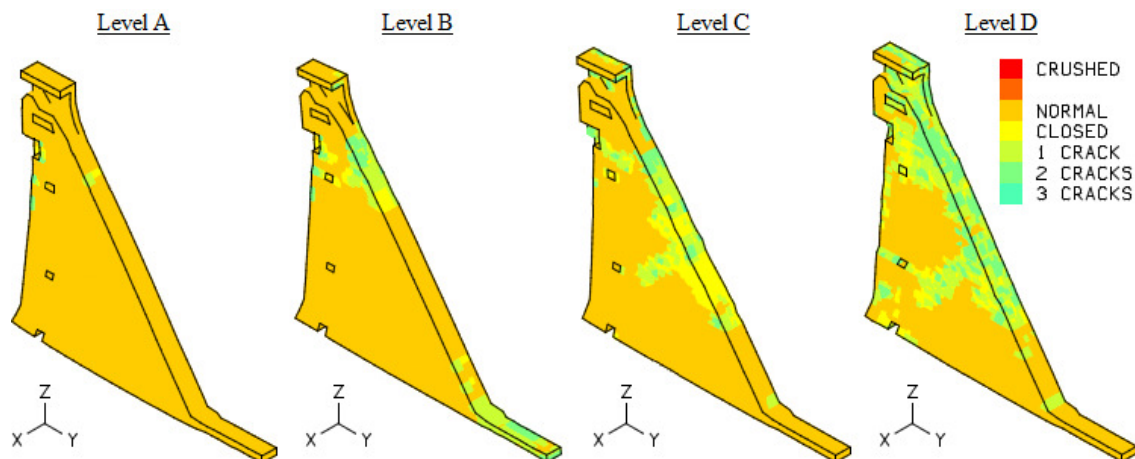


**Figure 4.2.** Accumulated damages at the central block from different seismic levels.

### Seismic level D

Excessive disruptions at the crest and the upper third of the wall are observed in the middle four block of the wall. Flooding at machine hall and inspection gallery is expected. Another crack passing through the whole cross section of the wall is formed at the lower part of the dam, horizontal to the downstream side, up to the first inspection gallery upward and perpendicular to the downstream side after it. Damage at the base of the upstream side, near the grouting curtain could be also observed.

Increased filtration is expected eventually reaching the injection gallery. The dam is severely damaged, the galleries in the dam are expected to be flooded and the dam body is separated in various detached parts in the central blocks. Due to quantity of damages accumulated in the entire wall and the increased danger of total collapse, the wall is classified as **DL4**.

### 4.3. Detached Part Stability and Post-earthquake Assessment

The results from the dynamic analyses for the selected seismic levels showed that the lowest seismic level that could cause a crack passing through the whole cross section of the dam is level B (MCE). This crack will result in detaching of the upper part of the dam wall. The global stability of this detached part will have major influence on eventual uncontrolled discharge of uncontrolled water quantities.

#### 4.3.1. Pseudo-dynamic post-earthquake stability assessment of the detached fragment.

Primarily a simplified manual pseudo-dynamic calculation is performed to assess the safety factors for sliding and overturning of the detached part for both observed cracks (horizontal and bi-linear). This calculation is based on equilibrium equations between active (hydrostatic/hydrodynamic) and retentive (frictional) forces.

Sliding of the detached part for bi-linear crack (at upstream direction):

$$k_s = \frac{H_\mu + F_w}{H_{EQ}} \quad (4.1)$$

If the safety coefficient  $k_s=1$  the horizontal acceleration which will cause the slide of the block is:

$$H_{EQ} = H_\mu + F_w = 3030 + 1454 = 4484 \text{ kN}; \quad a_g = \frac{H_{EQ}}{m} = 8,71 \text{ m/s}^2 = 0,89 \text{ g}$$

Overturning of the detached part for bi-linear crack:

$$k_o = \frac{(F_{sw} \Delta_1 + F_w \Delta_2)}{H_{EQ} \Delta_3} \quad (4.2)$$

Where  $\Delta_1$ - $\Delta_3$  are distances of acting forces to point A (Fig. 4.3.)

$$H_{EQ} = \frac{(F_{sw} \cdot \Delta_1 + F_w \Delta_2)}{1 \cdot \Delta_3} = \frac{5050 \cdot 5,17 + 1454 \cdot 5,68}{1,10,71} = 3209 \text{ kN} \quad a_g = \frac{H_{EQ}}{m} = 6,23 \text{ m/s}^2 = 0,64 \text{ g}$$

Based on the dynamic analyses results the seismic amplification at level +46,30 is approximately 3, therefore at input acceleration from  $0,64/3 \approx 0,21\text{g}$ , the detached part will overturn at upstream direction.

Sliding of the detached part for horizontal crack (at downstream direction)

$$k_s = \frac{H_\mu}{H_{EQ} + F_w} \Rightarrow H_{EQ} = H_\mu - F_w = 2214 - 656 = 1558 \text{ kN}; \quad a_g = \frac{H_{EQ}}{m} = 4,14 \text{ m/s}^2 = 0,42 \text{ g}$$

Overturning of the detached part over point A for horizontal crack

$$H_{EQ} = \frac{(F_{sw} \cdot \Delta_1 + F_w \Delta_2)}{1 \cdot \Delta_3} = \frac{3690 \cdot 4,94 + 656 \cdot 3,82}{1,7,96} = 2605 \text{ kN} \quad a_g = \frac{H_{EQ}}{m} = 6,92 \text{ m/s}^2 = 0,71 \text{ g}$$

Based on the dynamic analyses results the seismic amplification at level +51,90 is approximately 3, therefore at input acceleration from  $0.42/3 \approx 0.14g$ , the detached part will slide at downstream direction.

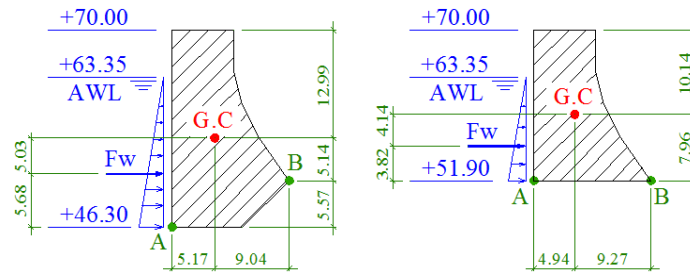


Figure 4.3. Scheme for the stability checks of the detached fragment of the wall.

#### 4.3.2. Numerical simulation of post-earthquake detached fragment response.

The pseudo-dynamic stability calculations performed in 4.3.1. use conservative approach as it does not considers the excitation duration, the fact that it is cyclic load and the energy needed for large displacements/rotations of the detached part. Therefore another, more realistic approach for the stability of the detached part is adopted (Wieland 2000, Malla 2003). The seismic response of the detached fragment is presented by nonlinear dynamic analysis, using contact elements for simulation of the interaction between detached part and the rest of the wall.

The stability of the detached fragment is performed for a seismic level B (MCE) using 2D model of a central block. The smeared crack model is a powerful tool for prediction of a crack location and crack propagation path. However due to the inability of this approach to perform physical discontinuity in the numerical model at the crack location it is difficult to accurately evaluate the global stability of a fragment – completely detached from a structural system. Therefore in the stability assessment of the detached part of the dam the crack is presented discretely. The seismic impact simulates an aftershock with magnitude comparable to the main excitation, which is a conservative assumption. Four dynamic analyses are performed, varying the crack pattern with the water level. Two different crack patterns are assumed, based on the results for seismic level MCE – horizontal and bi-linear crack. Two water levels are selected: average water level, assuming immediate aftershock and water level below the crack. Hydrostatic uplift acts on the detached part in case of average water level. The value of friction coefficient for concrete on concrete is accepted 0,6 considering wet crack surfaces.

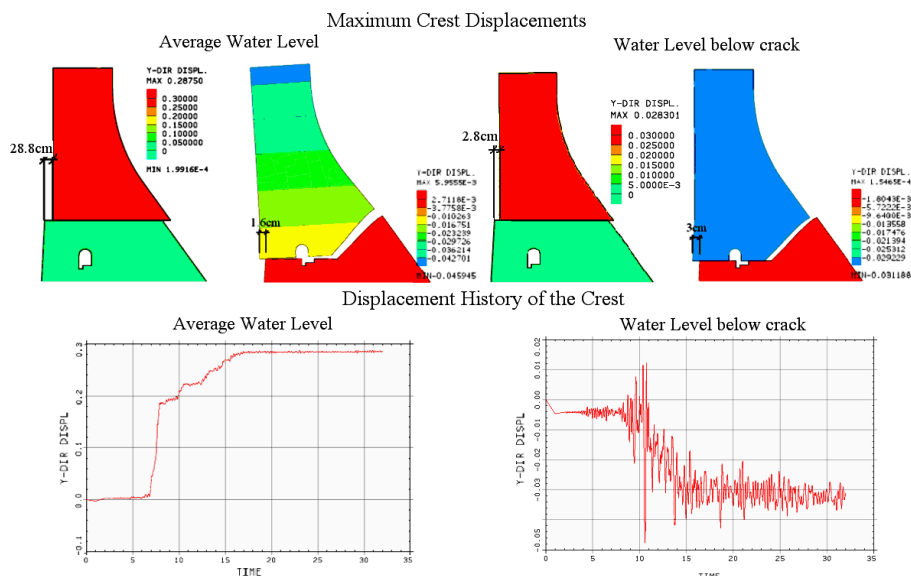


Figure 4.4. Aftershock response of the detached part of the crest for Seismic level B (MCE)

During the analyses no overturning threat was recognized for both types of detached fragments and both water levels. The maximum rotational displacements for the top of the crest were less than 3 cm. Sliding was recorded in all four analyses, as the maximum sliding displacement occurred in case of horizontal crack and average water level – around 30 cm, see Fig. 4.4. This displacement represents less than 3% of the cross-section width at the crack elevation, therefore the stability of the fragment is assured. For the rest of the analyses the maximum sliding displacements can be considered negligible – between 1,6 and 3 cm. The results demonstrate that although vastly damaged the dam crest is not losing overall stability and therefore uncontrolled water discharge is excluded in case of seismic level MCE.

## 5. CONCLUSIONS

Seismic assessment of a typical concrete gravity dam is performed for various predefined Seismic levels based on the Seismic hazard assessment of the region. The seismic excitation matches the uniform hazard acceleration response spectrum for given return period. The nonlinear behaviour of concrete is accounted and damage states are “rated” based on predefined Damage Levels (DL) according to their safety significance. Subsequent post-earthquake analysis of the damaged state of the structure are carried out and based on the results the following conclusions can be summarized:

- the structure remains practically elastic in case of Seismic level A (OBE);
- the lowest seismic level that might cause a crack through the whole cross section is level B (MCE);
- although pseudo-dynamic calculations showed possibility of sliding/overturning of the detached fragment, its overall stability was proved by dynamic contact analyses in case of seismic level B (MCE);
- severe damages are expected in the dam in case of Seismic levels C and D, including cracks through the dam’s cross section at various locations.

## ACKNOWLEDGEMENT

The authors wish to express their gratitude to Dr. Netzo Dimitrov from Risk Engineering Ltd, Dr. Dimitar Stefanov from Bulgarian Academy of Sciences and Dr. Dimitar Kislyakov from UACEG Sofia, for their valuable advices and support. The current paper is dedicated in memory of Dr. Christo Abadjiev, Professor Emeritus, UACEG Sofia, for his priceless guidance and mentoring in the field of Large dams.

## REFERENCES

- Campbell, K. and Bozorgnia, Y. (2010). A Ground Motion Prediction Equation for the Horizontal Component of Cumulative Absolute Velocity (CAV) Based on the PEER-NGA Strong Motion Database. *Earthquake Spectra, EERI*, Vol 26, No. 3, p. 635–650.
- F.E.R.C. (1999). Engineering Guidelines for the Evaluation of Hydropower Projects, Chapter 11 - Arch dams. Washington, USA.
- F.E.R.C. (2002). Engineering Guidelines for the Evaluation of Hydropower Projects, Chapter 3 - Gravity dams. Washington, USA.
- Kostov, M. (2005). Site specific estimation of Cumulative Absolute Velocity. *Proc., 18th International Conference on Structural Mechanics in Reactor Technology (SMiRT 18)*, Beijing, China, 3041–3050.
- Kostov, M. (2011). Seismic Safety Evaluation Based on DIP. *Proc., 21th International Conference on Structural Mechanics in Reactor Technology (SMiRT 18)*, New Delhi, India.
- Malla, S. and Wieland, M. (2003). Simple model for safety assessment of cracked concrete dams subjected to strong ground motions. *Proc. 21<sup>st</sup> ICOLD Congress*, Montreal, Canada, 151-165.
- SOLVIA (2003) Finite Element System - Version 03 - User Manual. SOLVIA Engineering AB, Vasteras, Sweden.
- U.S.N.R.C. (1997). Preearthquake planning and immediate nuclear power plant operator postearthquake actions. Regulatory Guide 1.166, Washington, USA.
- Wieland, M. and Malla, S. (2000). Earthquake safety of an arch-gravity dam with a horizontal crack in the upper portion of the dam. *Proc. 12-th World Conference on Earthquake Engineering*, Auckland, New Zealand.